ELSEVIER

Journal of Applied Geophysics 50 (2002) 319–331

JOURNAL OF APPLIED GEOPHYSICS

www.elsevier.com/locate/jappgeo

Electrical resistivity borehole measurements: application to an urban tunnel site

A. Denis *, A. Marache, T. Obellianne, D. Breysse

Centre de Développement des Géosciences Appliquées (C.D.G.A.), Recherche Geologie, B.18, Université Bordeaux 1, Avenue des facultés, 33405 Talence Cedex, France

Received 15 February 2001; accepted 2 April 2002

Abstract

This paper shows how it is possible to use wells drilled during geotechnical pre-investigation of a tunneling site to obtain a 2-D image of the resistivity close to a tunnel boring machine. An experimental apparatus is presented which makes it possible to perform single and borehole-to-borehole electrical measurements independent of the geological and hydrogeological context, which can be activated at any moment during the building of the tunnel. This apparatus is first demonstrated through its use on a test site. Numerical simulations and data inversion are used to analyse the experimental results. Finally, electrical resistivity tomography and single-borehole measurements on a tunneling site are presented. Experimental results show the viability of the apparatus and the efficiency of the inverse algorithm, and also highlight the limitations of the electrical resistivity tomography as a tool for geotechnical investigation in urban areas.

Keywords: Resistivity tomography; 2-D inversion; Tunnel boring; Geotechnical investigation

1. Introduction

Traditionally, a geotechnical investigation along a tunnel axis is based on destructive borings, pressuremeter profiles and drilling in order to obtain samples ready for laboratory tests. Contractors do not usually look for small obstacles or slow longitudinal variations in soil properties along the tunnel axis. In fact, they accept the risk to hit such an obstacle with the head of the tunnel boring machine, because the time to discover all small obstacles in the path of the tunnel boring machine may be prohibitively high. Without a priori information on the site, the probability of meeting an obstacle is often too low to justify geophysical surveys. Single and borehole-to-borehole electrical measurements are more rarely performed during a geotechnical investigation for buildings on an urban tunnel than in mineral exploration (Spies, 1996). However, since a longitudinal geological section can easily fail in a heterogeneous soil, the project manager may prefer to focus on specific sections where, for instance, severe changes in permeability or nature of the soil are present. Indications of geological variations are first provided by the examination of cuttings, using mechanical parameters, such as the advance rate recorded during boring. Thus, when severe geological changes are identified in the path of the tunnel boring

* Corresponding author. Tel.: +33-5-56-84-29-19; fax: +33-5-56-80-71-38.

E-mail address: adenis@cdga.u-bordeaux.fr (A. Denis).

0926-9851/02/$ - see front matter
PII: S0926-9851(02)00150-7

machine, the project manager can quickly request more information about the geological environment. In this case, electrical resistivity surveys can be a useful tool to help the project manager detect geological variations. In order to be of practical use, the electrical resistivity measurements should not slow down the tunnel boring machine. From a cost point of view, any unforeseen delay in the tunnelling cannot be accepted. The subsurface geological section in the area of an urban tunnel is often investigated by many and densely distributed drill holes, with a spacing about 30 to 50 m. The basic idea is then to utilize such holes but now for electrical surveys with permanent electrodes.

This paper describes how wells drilled during the geotechnical investigation can be used to carry out electrical measurements in the path of a tunnel boring machine. A specific experimental apparatus for electrical measurement into a borehole is first presented. Then, experimental results from a test site are analysed, using numerical simulations and data inversion, to obtain a 2-D image of the resistivity. Finally, electrical measurement results from a tunnelling site located south of Paris (France) are presented. Results demonstrate the limits of using electrical resistivity tomography for a geotechnical investigation in an urban area.

2. Methodology

One way to save time in electric borehole geophysics is to re-use boreholes previously drilled for geotechnical investigations. At the end of the geotechnical investigation, each well is equipped with stainless steel electrodes. The well-equipment consists of a PVC tube on which metallic circular rings are fixed at different levels (Bevc and Morrison, 1991, Daily and Ramirez, 1999). The configuration is different above and below the water table (Fig. 1). Into the unsaturated zone, a grout cement case ensures the contact between the soil and the electrodes. Under the water table, the well plastic tube is pierced and contact is made through a filling of sand and gravel. These wells are open at the bottom for use in water level measurement. These permanent electrodes are only activated if the project manager requires more information when the tunnel boring machine is close to these holes (Denis et al., 2000).

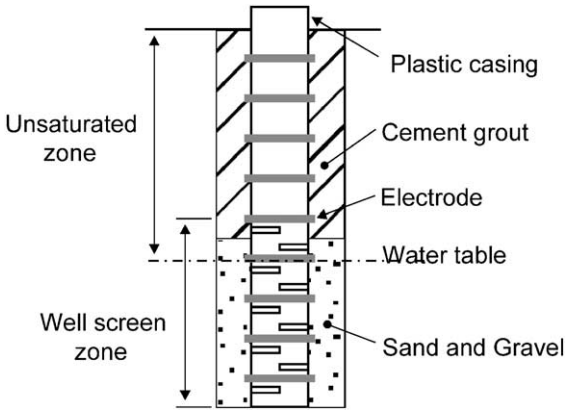

Fig. 1. Diagram showing the measurement system.

As the electrical devices must stay in the soil for a long time, it is important to ensure that the cement grout does not disturb the potential field. The magnitude of its effect can be studied from a numerical simulations based on the work of Wait (1982). The current point source I is located at the borehole origin. The interior region ($r<a$) is homogeneous and has resistivity ρ_{Grout}; the exterior region ($r>a$) is also homogeneous and has resistivity ρ_{Soil}. It is further assumed that the borehole is of infinite length. Hence, in the case of single-borehole electrical measurements, the interior potential at a point M located at depth z from the origin is

$$V_{\text{M}} = \frac{I\rho_{\text{Grout}}}{2\pi^2}\int_0^{\infty} [K_0(\lambda r) + A(\lambda)I_0(\lambda r)]\cos(\lambda z)\mathrm{d}\lambda$$

where

$$A(\lambda) = \frac{-\lambda a(K-1)K_0(\lambda a)K_1(\lambda a)}{1+\lambda a(K-1)I_0(\lambda a)K_1(\lambda a)}$$

and

$$K = \frac{\rho_{\text{Grout}}}{\rho_{\text{Soil}}}$$

Here I denotes the intensity of the current, λ denotes the integration variable and $K_0(x)$, $K_1(x)$ and $I_0(x)$ denote the three different Bessel functions, respectively.

Single-borehole electrical measurement requires $r=0$, hence we obtain the following expression for the interior potential:

$$V_M = \frac{I\rho_{Grout}}{4\pi z} + \frac{I\rho_{Grout}}{2\pi^2}\int_0^\infty A(\lambda)I_0(0)\cos(\lambda z)\mathrm{d}\lambda$$

In the case of electrical resistivity tomography, the exterior potential can be calculated at a distance r and depth z from the origin using following relation:

$$V_M = \frac{I\rho_{Grout}}{2\pi^2}\int_0^\infty B(\lambda)K_0(\lambda d)\cos(\lambda z)\mathrm{d}\lambda$$

where

$$B(\lambda) = \frac{1}{1+\lambda a(K-1)I_0(\lambda a)K_1(\lambda a)}$$

By applying these equations, we can study the effect of the contrast between the cement grout and the adjacent soil, considered to be homogeneous, on single and borehole-to-borehole electrical measurements. An example application is presented in the following section.

3. Application to a test site

Before using this methodology for a tunnel site, one has to examine the validity of the methodology. For this purpose, three wells (A, B and C) were drilled to depths ranging from 3.3 to 3.8 m. Distances between the boreholes ranged from 5 to 15 m (Fig. 2). The geological model of the test site, Fig. 2, is based on visual observations made during drilling. In boreholes A and B, two successive layers were detected and only one in borehole C. For A and B, there is a dry sand and gravel layer up to a depth of 1.50–1.60 m, and then a wet sand layer. For C, the sand layer is observed all along the borehole length with increasing moisture with depth. The water table is about 6 m deep.

Ten electrodes were set up to a depth of 3.25 m into each borehole at 25 cm spacing. The first electrode was set up at a depth of 1 m. The cement casing (ASTM type I Portland cement) was mixed with water at a ratio of 2:1 by weight. Laboratory measurements were made to determine the electrical properties of the grout. Electrical data measurements were carried out for different periods on four samples. The measured resistivity, after about 20 days, was about 40–50 Ohm m. Beyond 20 days, the softly moist grout showed an increased resistivity, up to 100 Ohm m.

From the equations provided in the previous section, the effect of the cement grout on single-borehole and borehole-to-borehole electrical measurements can be estimated. It appears that, for an idealised condition (circular diameter: a = 0.15 m and no infiltration of the grout into the formation), the effect is more important

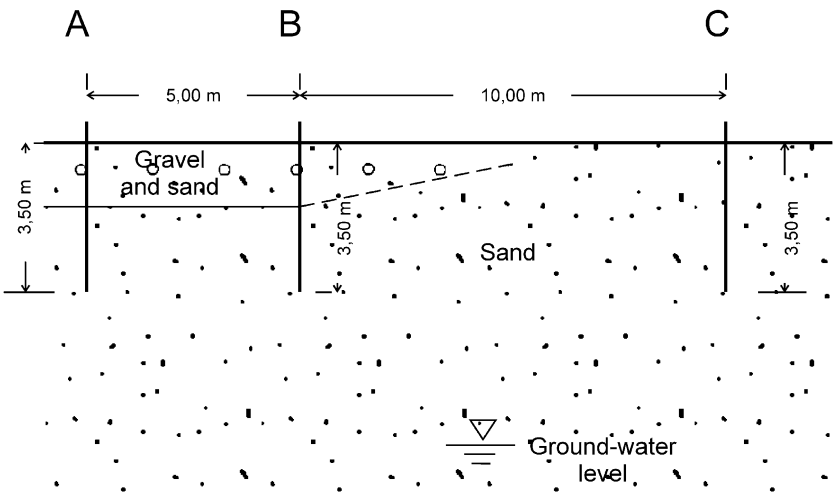

Fig. 2. Shallow geological section and borehole arrangement for the test site.

on a single-borehole than on borehole-to-borehole electrical measurements (Figs. 3 and 4). In the case of low grout over soil resistivity ratio, care must be taken while inverting the data. The resistivity of the grout should be introduced in an initial model for the inversion scheme. It may be noted that a part of this effect is also due to the presence of the grout close to the current electrode, the effect of which cannot be entirely accounted for by the image-point method.

3.1. Numerical simulations and data inversion

The numerical simulations and inversion scheme used to analyse experimental data are presented in the following. The interpretation of DC apparent resistivity data collected over a complex earth structure is usually performed using forward and inverse modelling. A synthetic example of forward and inverse modelling, using single-borehole electrical measurements, is first presented, and then a practical method for reconstructing 2-D resistivity distribution using borehole-to-borehole electrical measurements is described.

Numerical simulations were performed using a 3-D finite-element method (CESAR LCPC Software). A brief description of this technique, which has been described extensively (Zienkiewicz, 1973; Murai and Kagawa, 1985), is presented first. The FEM treats the problem by discretizing the terrain into homogeneous blocks called finite elements. Galerkin minimisation and Dirichlet and Newman boundary conditions, where appropriate, are applied to every element. The individual element equations can then be assembled into one global system where the nodal potential vector is the unknown. The global system is solved and the nodal potential is obtained. The potential distribution is then converted into apparent resistivity values.

Many inversion schemes are available (Daily and Owen, 1991; Shima, 1992; Dabas et al., 1994; Loke and Barker, 1996a,b; Labrecque et al., 1996; Mauriello and Patella, 1999; Abubakar and Van den Berg, 2000). Most of them are iterative and require regularization techniques (Tikhonov and Arsenin, 1976) either by truncation (zeroing elements of the matrix), by reducing the effect of undetermined parameters (damping factor) or by a smoothness criterion (Dabas et al., 1994).

A numerical example of the FEM simulation of single-borehole electrical measurements then inverted by a classical fully nonlinear method (Loke and Barker, 1996a) is displayed in Fig. 5. The model is a two-layer earth model: the upper layer has a resistivity of 20 Ohm m and the second layer of 100 Ohm m. The thickness of the upper layer is 1.5 m. The first electrode is located at a depth of 1 m.

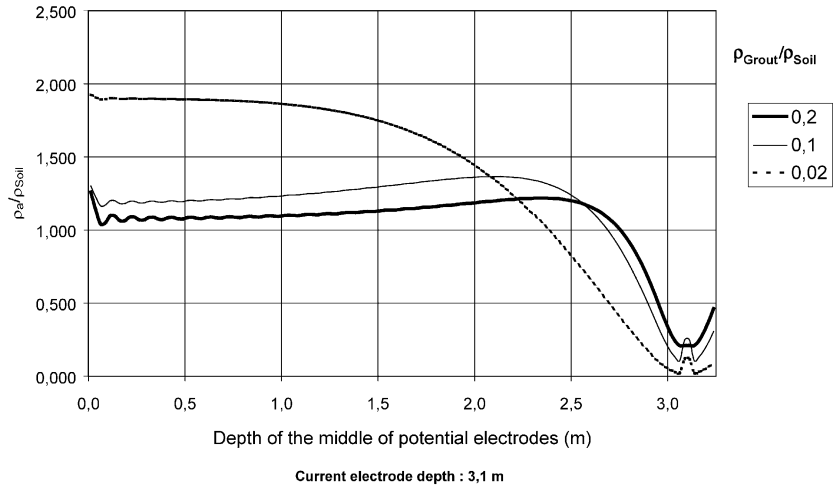

Fig. 3. Example of the effect of the cement grout on single-borehole measurements.

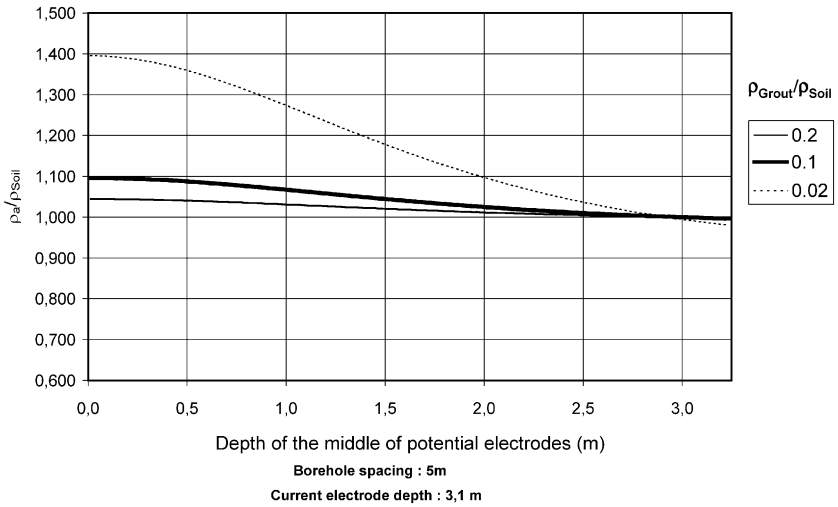

Fig. 4. Example of the effect of the cement grout on borehole-to-borehole measurements.

The interpretation of single-borehole electrical measurements, in the case of horizontal layering model, is straightforward.

For borehole-to borehole electrical measurements we implemented an inverse method based on the double constraint method (Wexler et al., 1985). In this method, the FEM forward modelling is first constrained with the known current source value, and the current density is calculated in each element. Then, the FEM is constrained with the measured voltage and the current source value as the voltage gradient in each element is calculated. Based on these calculations the resistivity of each element is determined. Instead of a FEM forward modelling, we proposed to calculate the current density in each element by an analytical relationship using measured apparent resistivity and the total current flowing through the current electrodes. In this case, the basic principle is, then, that the sets of current flow pattern are not highly affected by the distribution of electrical resistivity.

The region of interest is, between two boreholes, subdivided into a 2-D grid. For each excitation (j), the total current flowing through the electrodes (Ij) and voltages at each potential electrodes are measured. Assuming initially an isotropic homogeneous medium (with an apparent resistivity ρ_a), the current flux density $\bar{J}$ (A/m^2) and the electric field intensity, $E = -\nabla\phi$, at the location corresponding to the potential electrodes, are calculated. From these values, the current flux density $\bar{J}_i$ can then be estimated as well as the electrical field intensity $\bar{E}_i$ distribution along each current flow within each element. This procedure is repeated for all excitations. Results are stored for each

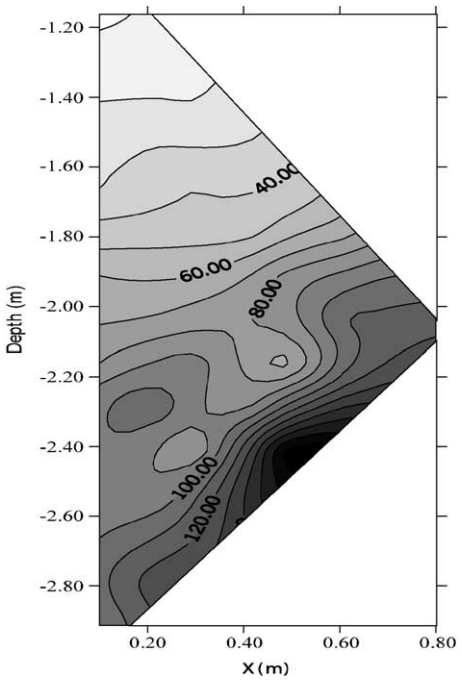

Fig. 5. Inversion result obtained from a single-borehole pole–dipole configuration.

element of the grid affected by the current flow-line pattern. With $\bar{J}_i$ and $-E_i$ available for each element, Ohm's law is generally not satisfied. Hence, the minimisation of the square of the residual of each element and for all excitation is sought by adjusting the resistivity (ρ_i) within each element. This procedure yields:

$$\rho_i = \frac{\sum_{j=1}^{X(i)} \nabla\phi_{ij} \cdot \nabla\phi_{ij}}{\sum_{j=1}^{X(i)} \bar{J}_{ij} \cdot \nabla\phi_{ij}}$$

which is the estimation of the resistivity within element i. Here $X(i)$ represents the number of excitations over which the sum is taken for element i.

As synthetic example, the same two-layer earth model described previously, yet with different resistivity values, is used to represent the survey area. The resistivity of the upper layer is 100 Ohm m, while for the second layer (half-space) resistivity is 20 Ohm m. The thickness of the upper layer is again 1.5 m and the distance between boreholes is 5 m. The apparent resistivity responses have been computed by using 3-D finite elements. The inverted model is shown in Fig. 6a. It can be observed that the true resistivity for the upper layer is underestimated while the estimation for the second layer is accurate. Fig. 6b shows the number of excitations over which the estimation of the resistivity within each element is carried out. As can be seen from this figure, the number of current flow-line pattern is low along the boundaries of the region of interest. By comparing the true resistivity of the earth model and the resistivity of the inverted model, a model misfit, Mi, using the following relation, can be calculated:

$$\mathrm{Mi} = \frac{(\rho_{\mathrm{true}(i)} - \rho_{\mathrm{inv}(i)})}{\rho_{\mathrm{true}(i)}} \times 100\%.$$

The percent of rms error in the model or rms misfit M (Olayinka and Yaramenci, 1999, 2000), by considering the entire model, can be calculated from:

$$M = \left[\frac{1}{\mathrm{NC}} \sum_{i=1}^{\mathrm{NC}} \mathrm{Mi}^2\right]^{\frac{1}{2}}$$

where NC is the total number of blocks; $\rho_{\mathrm{true}(i)}$ is the actual model resistivity and $\rho_{\mathrm{inv}(i)}$ is the resistivity of the ith block in the inverted model.

The misfit in contoured model (Fig. 6c) shows that underestimation of the true resistivity is greatest around the horizontal contact of the two layers. The model rms misfit M is about 29%; this value is in agreement with results given by Olayinka and Yaramenci (2000). Moreover, these authors have also demonstrated that the distribution of misfit (Mi) is rather concentrated in some specific regions, notably the contacts.

Although the inversion method does not use the exact current flow path, the result obtained from this synthetic example seems to be robust. In the following, borehole-to-borehole electrical measurements will be inverted by this method and single-borehole measurements by a classical fully nonlinear method.

3.2. Experimental results and discussion

Several electrical measurements were performed at this testing site. The vertical electrodes were used for single-borehole and cross-borehole measurements in a pole–dipole configuration. All of them were measured 1, 2 and 3 months after the well was cased. A very good reproducibility of the results has been observed. Results from single-borehole electrical surveys (Fig. 7) can be attributed to a succession of two high-resistivity layers, the upper with a resistivity between 800 and 1000 Ohm m, and the lower with a resistivity of 200 Ohm m for boreholes A and B. The resistivity of this layer on the borehole C decreases from 500 to 200 Ohm m along the depth. As the grout resistivity is close to 100 Ohm m, the ratio of the grout resistivity over the soil resistivity is larger than 0.08. Thus, experimental data can be used without correction.

In order to obtain a 2-D image of the resistivity structure between boreholes, a total of 200 measurements were taken between each of the current and potential electrode pairs. For the inversion, based on the double constraint method, 50 elements were used between boreholes A and B. Fig. 8 shows the final reconstructed image. This figure suggests that the zone between 0 and 1.3 m with resistivity values ranging from 500 to 200 Ohm m can be interpreted as the gravel layer. The lower zone with values below 200 Ohm m corresponds to the sand layer.

Three months later, in the absence of any strong rains, a third well (C) was drilled. Distances between

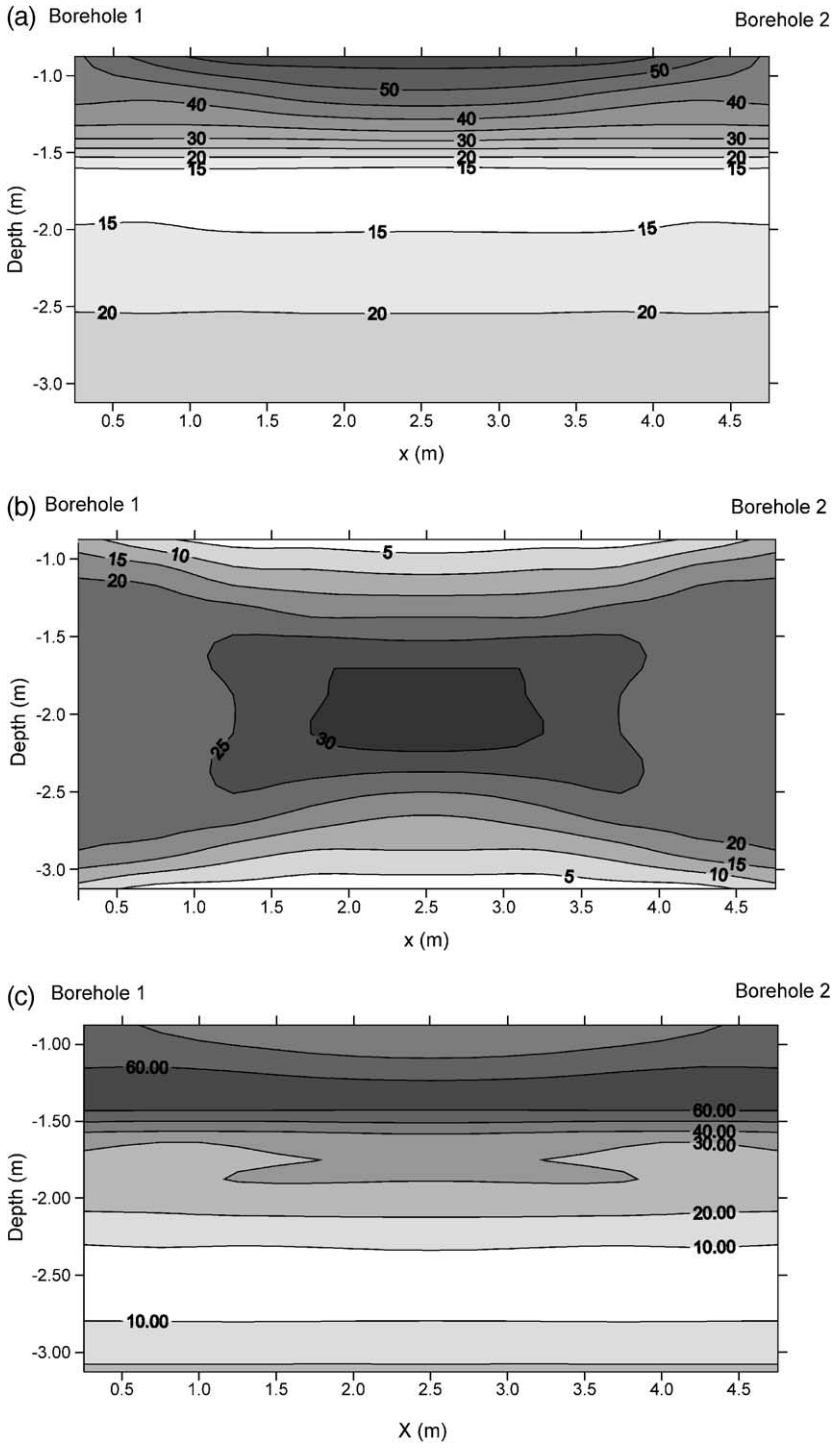

Fig. 6. Resistivity models obtained by inverting the synthetic data. (a) Inverted model. (b) Number of current lines flowing through per cell. (c) Model misfit between true resistivity and inverted data (a).

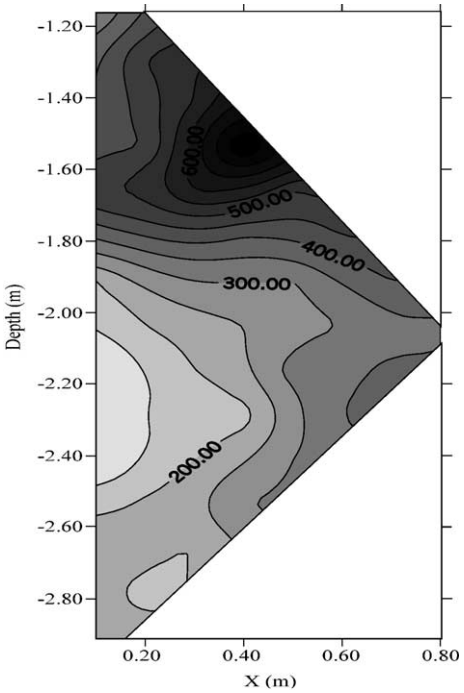

Fig. 7. Inversion results obtained from the borehole A.

the other boreholes were 15 and 10 m, respectively, for A and B (Fig. 2). Fig. 9 shows a plot of the resistivity distribution obtained after data inversion, between A–B and B–C. It can be observed that the reconstructed image between A and B is quite similar to that presented in Fig. 8. We observe that the resistivity values of the upper layer (gravel layer) are between 500 and 1900 Ohm m and between 150 and 500 Ohm m for the lower layer. This strong increase in the resistivity values is due to the decrease of the soil moisture between the two surveys. The right part of the reconstructed image (tomography B–C) suggests that the upper layer between B and C disappears progressively. The zone, close to borehole C, with resistivity value ranging from 400 to 600 Ohm m, can be interpreted as a single sand layer. Moreover, one can observe the lateral resistivity variation for the lower layer as if the upper layer was protecting against modification of the soil moisture between A and B. From such interpretations, a geophysical model can be built which fits the shallow stratigraphic section of the test site very well. The well-equipment and cross-borehole inversion method seem efficient and robust. They can indeed be used on a real geotechnical site.

4. Application to a tunneling site in an urban area

4.1. Description of site

Five boreholes were drilled up to 30-m depth on average. The distance between wells ranges from 11 to 90 m (Fig. 10a). On the last 15 m, wells were equipped with 15 electrodes placed at every meter and

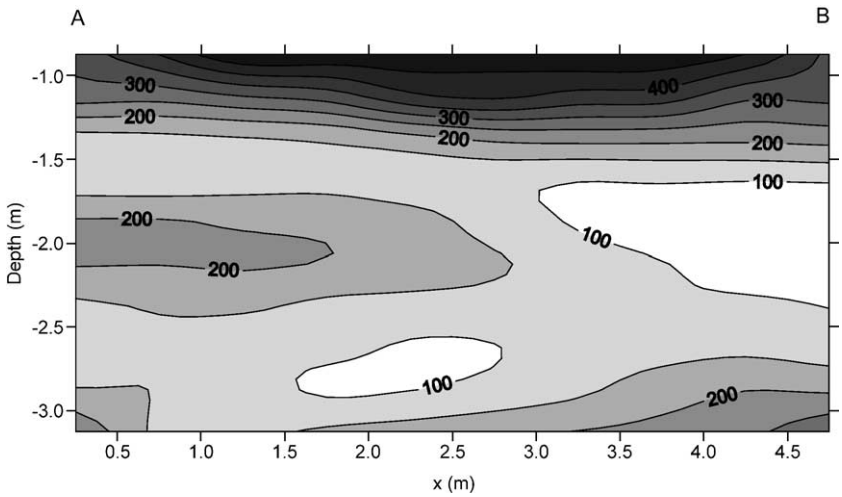

Fig. 8. Reconstructed two-dimensional resistivity image between boreholes A and B.

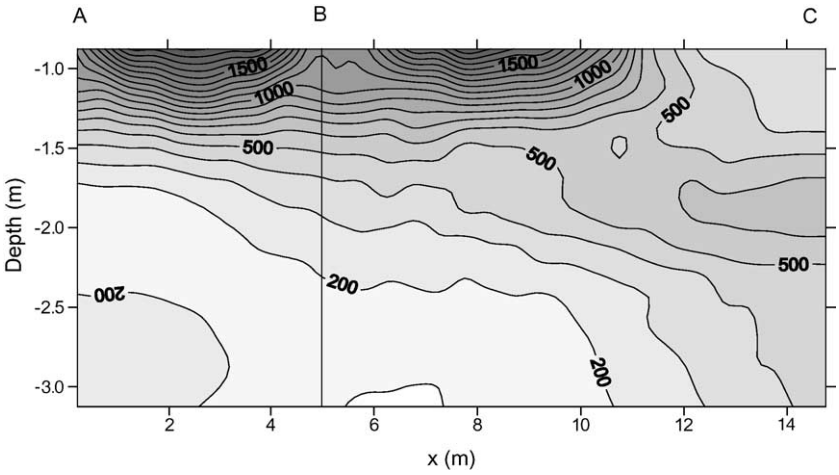

Fig. 9. Reconstructed two-dimensional resistivity image between A–B and B–C after 3 practically dry months.

fixed around a cylindrical support in PVC pipe as described previously. A cement grout was injected to ensure a good coupling between the electrodes and the soil. A shallow stratigraphic log of the site appears to indicate 3.5 m of marl, 6 m of plastic clay and 5.5 m of thick chalk in the region of interest, i.e. between 15 and 30 m (Fig. 10b). In this survey site, the tunnel (3 m in diameter) was drilled at 22.7-m depth into the clay layer.

4.2. Experimental results and limits

Single-borehole measurements were made at this site using a pole–dipole array (allowing to emphasize resistivity contrasts), and cross-borehole measurements using a pole–pole array (allowing to obtain less noisy results for large distance between wells).

The single-borehole measurements had a good signal-to-noise ratio and the nonlinear 2-D inversion could be applied successfully. On the contrary, the borehole-to-borehole measurements were very noisy and the nonlinear inversion did not converge, not even when using the more robust L1-norm, i.e. minimizing the absolute difference between measurements and calculated response. However, the approximate double constraint method produced results also in the case of the noisy borehole-to-borehole measurements, and was thus chosen to be presented with the synthetic examples and used on the field measurements at the tunnel site.

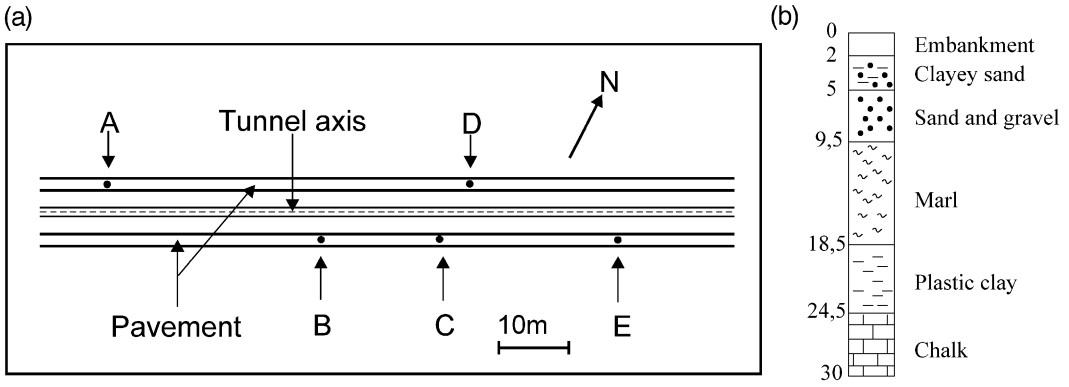

Fig. 10. Borehole arrangement and geology for the tunnel site investigation. (a) Boreholes arrangement. (b) Shallow stratigraphic section.

From single-borehole data, the apparent resistivity values are calculated, plotted on a pseudosection and then inverted. From cross-borehole data, the aim is to realise a reconstructed two-dimensional resistivity image between each couple of boreholes using the inversion algorithm described in the previous section.

For the project manager the objectives were to determine the depth to the top of the chalk basement and the homogeneity of the clay. Since electrodes ranged from 15 to 30 m, it can be expected to detect layer limits as marl–clay and particularly clay–chalk because the last one presents enhanced resistivity contrast. Some local heterogeneities may also be detected.

Fig. 11 shows an example of the resistivity image obtained by inverting single-borehole observed measurements. Globally, the resistivity values indicate a low resistivity soil. A relatively homogeneous environment up to 25–26 m can be noted, and then the resistivity increases further. This zone corresponds to the clay–chalk transition. One can also observe a more resistant area around 20 m deep, which can be interpreted as a small sandy layer within the clay. As expected, this area appears weakly on the reconstructed two-dimensional resistivity image (Fig. 11).

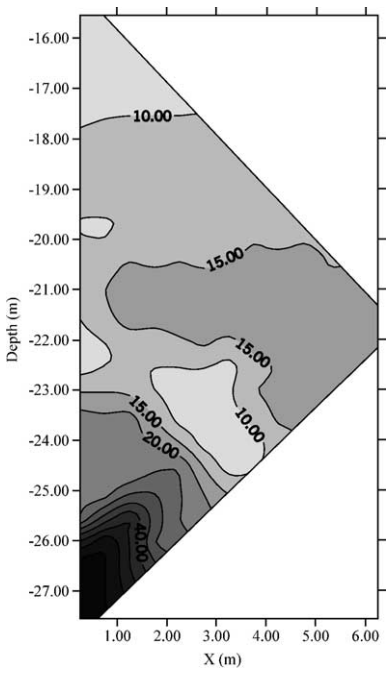

Fig. 11. Example of reconstructed image from single-borehole measurements (borehole A).

An example of reconstructed two-dimensional resistivity image between D and E obtained from algorithm inversion is shown in Fig. 12. A total of 450 measurements was taken for each pair of boreholes and 100 cells were used for the inversion method based on the double constraint method. As can be seen from this figure, the average resistivity value is lower than that obtained from single-borehole measurements, because, first, the investigated volume increases with distance between boreholes and the marl located above has an effect on the measurements, and second, a pole–pole array was used. We can again observe a significant increase in the resistivity gradient as a function of depth after 25 m (clay–chalk limit). Furthermore, one can note a decrease in resistivity from D to E up to 10 m from D, which could be interpreted as a lateral variation of facies. Using the same wells, basic geotechnical investigations should detect this variation between D and E but they cannot indicate how such a longitudinal change occurs. From D to E, the top of the chalk layer shows a low angle dip.

Remarks on the limitation of the electrical methods in an urban area are given below.

(a) The reconstructed resistivity image obtained from single-borehole measurements can show local anomalies (cavity or block) but it is impossible to locate them with respect to the azimuth.

(b) In electrical resistivity tomography, all source–receiver combinations are performed. For each combination, the measurement result is an average of three successive shoots. The measurement apparatus calculates parameter q (%) correlated to the variability of the three shoots (q increasing with error). The relative deviation q, also called the coefficient of variation, is the ratio of the deviation to the mean; q is defined as:

$$q = \frac{\left(\sum_{i=1}^{k} (m_i - m)^2\right)^{1/2}}{m}$$

where k is the number of shoot, m_i denotes the ith measurement and m denotes the mean of the k measurements.

For each cross-borehole an average q is calculated (Fig. 13). As can be seen from this figure, factor q

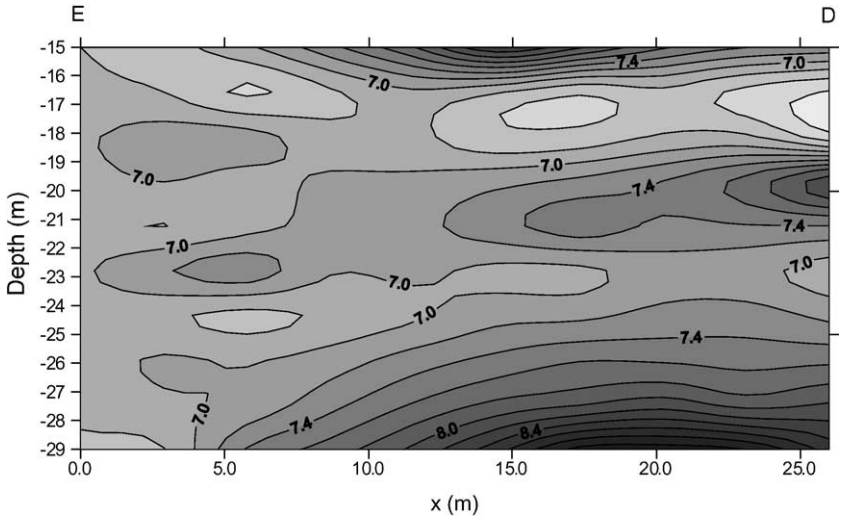

Fig. 12. Reconstructed two-dimensional resistivity image between D–E using a pole–pole array.

increases with distance, proving the decrease of measurement repeatability with distance between wells increases. This parameter gives a global evaluation of the repeatability of measurements but no information on their quality. In this study, we expected to obtain data up to 90 m (between A et E) but more and more observed measurements proved worthless with distance. Since the tunnel site was in an urban area, data could easily be contaminated by noise from other electric sources (e.g. power lines, leakage current) along the wires connecting the remote electrodes. In a recent paper, Bing and Greenhalgh (2000) show that the pole–pole array configuration is not the best choice because small voltages may easily be masked by underground noise. Our results seem to confirm their numerical simulations. It is not suitable to conduct such work in an urban area using a pole–pole array because of the two remote electrodes (Bing and

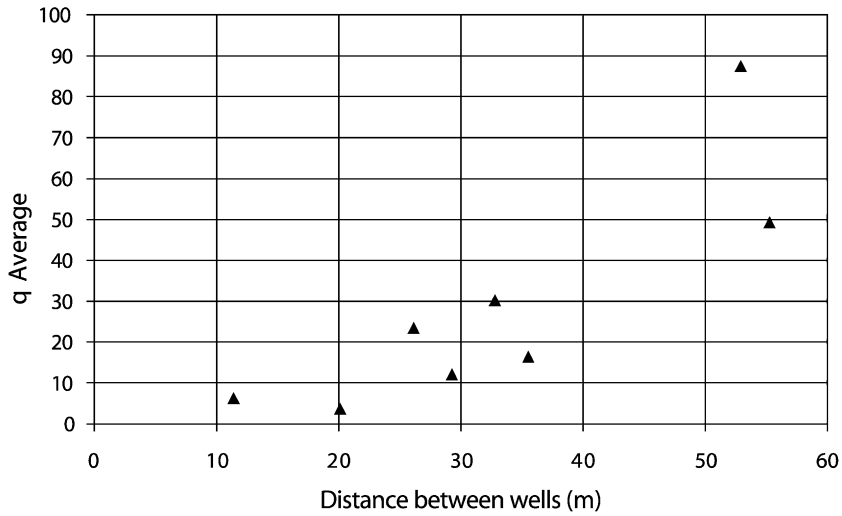

Fig. 13. Evolution of average q as a function of the distance between wells.

Greenhalgh, 2000). Pole–dipole or dipole–dipole configurations should be used in an urban area for electric resistivity tomography.

5. Conclusions

Using wells drilled during the geotechnical investigation of a tunnelling site to perform electrical resistivity measurements is an economically efficient way to complete the geological information on specific section which is reached by the tunnel boring machine. The multi-electrode well equipment must be set up after pressuremeter measurements or sampling for laboratory tests. The borehole can be kept as a piezometer and electrical measurements can be performed in the unsaturated zone as well as under the water table level. Furthermore, the described apparatus is low-cost and can be re-used at any time during the construction of an urban tunnel. Although many inverse algorithms are available, a noniterative inverse method for cross-borehole measurements was found to perform well. This method does not need an initial model, and provides a very fast and efficient two-dimensional reconstructed resistivity images between boreholes. Although this technique does not determine the exact current path to perform a resistivity reconstruction, the results obtained through numerical examples appear robust. Under further research, this technique can be easily improved by using electrical FEM forward simulation in order to consider the curved current path following the previously calculated resistivity distribution.

The single-borehole and cross-borehole direct current electrical measurements carried out in a test site show the viability of the multi-electrode device and the efficiency of the inverse algorithm. Results show that it is possible to detect some vertical and horizontal changes in the soil and a relevant physical property, i.e. soil moisture, as required by contractors on specific geological sections.

The first results obtained on a tunnelling site confirm the results obtained within the test site and provide the limits of the electrical resistivity tomography, using a pole–pole array for geotechnical investigation in an urban area. In this urban area, 40 m between two boreholes appears to be an appropriate limit above which one has to analyse the measurements more carefully. Electrical measurements complement the geological information between wells efficiently. Such information is important for the project manager because some severe changes in the nature of the soil can modify the rate and conditions of drilling advancement of the tunnel boring machine.

Acknowledgements

This study has been conducted in collaboration with BOUYGUES and Me2i companies and under the financial support of the Research Division (DRAST) of the French Ministry for Building and Transportation.

References

Abubakar, A., Van den Berg, P.M., 2000. Non-linear three-dimensional inversion of cross-well electrical measurements. Geophys. Prospect. 48, 109–134.

Bevc, D., Morrison, H.F., 1991. Borehole-to-surface electrical resistivity monitoring of a salt water injection experiment. Geophysics 56, 769–777.

Bing, Z., Greenhalgh, S.A., 2000. Cross-hole resistivity tomography using different electrode configurations. Geophys. Prospect. 48, 887–912.

Dabas, M., Tabbagh, A., Tabbagh, J., 1994. 3D inversion subsurface electrical surveying – I Theory. Geophys. J. Int. 119, 975–990.

Daily, W., Owen, E., 1991. Cross-borehole resistivity tomography. Geophysics 56, 1228–1235.

Daily, W., Ramirez, A.L., 1999. Electrical imaging of engineered hydraulic barriers. Geophysics 65, 83–94.

Denis, A., Marache, A., Breysse, A., Obéllianne, T., 2000. Reconnaissance à l'avancement des tunneliers. Plan Génie Civil, Rapport d'avancement Bouygues, Me2i, CDGA, No. 2.

Labrecque, D., Miletto, M., Daily, W., Ramirez, A.L., Owen, E., 1996. The effect of "Occam" inversion of resistivity tomography data. Geophysics 61, 538–548.

Loke, M.H., Barker, R.D., 1996a. Rapid least-squares inversion of apparent resistivity pseudosections by a quasi-Newton method. Geophys. Prospect. 44, 131–152;
Loke, M.H., Barker, R.D., 1996. Rapid least-squares inversion of apparent resistivity pseudosections by a quasi-Newton method. Geophys. Prospect. 32, 159–186.

Loke, M.H., Barker, R.D., 1996b. Practical techniques for 3-D inversion surveys and data inversion. Geophys. Prospect. 44, 499–523;
Loke, M.H., Barker, R.D., 1996. Practical techniques for 3-D inversion surveys and data inversion. Geophys. Prospect. 32, 159–186.

Mauriello, P., Patella, D., 1999. Resistivity anomaly imaging by probability tomography. Geophys. Prospect. 47, 411–429.

Murai, T., Kagawa, Y., 1985. Electrical impedance computed tomography based on a finite element model. IEEE Trans. Biomed. Eng. BME-32 (3), 177–184.

Olayinka, A.I., Yaramenci, U., 1999. Choice of the best model in 2-D geoelectrical imaging: case study from a waste dump site. Eur. J. Environ. Eng. Geophys. 3, 221–244.

Olayinka, A.I., Yaramenci, U., 2000. Assessment of the reliability of 2D inversion of apparent resistivity. Geophys. Prospect. 48, 293–316.

Shima, H., 1992. 2D and 3D resistivity image reconstructing using crosshole data. Geophysics 57, 1270–1281.

Spies, B.R., 1996. Electrical and electromagnetic borehole measurements: a review. Surv. Geophys. 17, 517–556.

Tikhonov, A., Arsenin, V., 1976. Méthodes de Résolution de Problèmes Mal Posés Editions Mir.

Wait, J.R., 1982. Geo-Electromagnetism Academic Press, Chap. 1, 67 pages.

Wexler, A., Fry, B., Neuman, R.M., 1985. Impedance-computed tomography algorithm and system. Appl. Opt. 24, 3985–3992.

Zienkiewicz, O.C., 1973. La méthode des éléments finis. Edisciences, 530 pages.